



Cite this: *Chem. Sci.*, 2024, **15**, 2990

All publication charges for this article have been paid for by the Royal Society of Chemistry

Received 23rd November 2023  
Accepted 15th January 2024

DOI: 10.1039/d3sc06299f  
[rsc.li/chemical-science](http://rsc.li/chemical-science)

## Introduction

Within the great variety in organometallic chemistry, cyclopentadienyls (Cp) are among the most common carbon-based ligands. While coordination compounds with lanthanide and main group elements are well studied, their original and still current domain is found for the transition metals with over 66 000 catalogued systems according to the Cambridge Crystallographic Data Centre (CCDC).<sup>1</sup> To a significant extent, this enormous number of structures is due to the adaptability of Cp-metal bonding to the chemical environment by diverse binding modes and hapticities ranging from  $\eta^1$  to  $\eta^5$ . Consequently, hundreds and thousands of examples for almost every transition metal exist with structurally defined cyclopentadienyl binding motifs. However, a considerable gap becomes apparent for the coinage metal (Cu, Ag, Au) cyclopentadienyls, due to their pronounced instability towards moisture, air and light, and even their thermal lability at ambient conditions. Thus, with only 47 hits according to CCDC in total, group 11 is the by far least structurally characterized transition metal group in this context.<sup>1</sup> Among these 47, the majority (39) belongs to copper complexes,<sup>2–9</sup> while silver<sup>10</sup> and gold<sup>11–17</sup> cyclopentadienyls are extraordinarily rare, with only one and seven structures, respectively.<sup>1</sup> For copper,  $\eta^5$ -coordination is observed exclusively (with two heterobimetallic exceptions)<sup>18,19</sup> as for example

in  $[\text{Cu}(\text{C}_5\text{H}_5)(\text{PPh}_3)]$ .<sup>4,5</sup> Silver, in comparison, may adopt  $\eta^5$  or  $\eta^3$  hapticities, both observed with  $[\text{Ag}(\text{C}_5(\text{SiMe}_3)_3\text{H}_2)(\text{P}^n\text{Bu}_3)]$ ,<sup>10</sup> while gold predominantly tends to  $\eta^1$  with distortions towards  $\eta^3$  as in  $[\text{Au}(\text{C}_5\text{Ph}_4\text{H})(\text{PPh}_3)]$ .<sup>11</sup> Moreover, there is no complete structurally comparable series known for group 11 cyclopentadienyl complexes at all, as either differing Cp substitution patterns or co-ligands exercise crucial influence on the bonding situation. In addition to this gap of knowledge regarding their structures, new synthetic approaches to metal Cp complexes with increased stabilities are needed. So far, attempts to overcome the stability issues have mainly focused on sterical shielding in combination with high electron affinity Cp derivatives, preventing oxidative decomposition. This was, for example, impressively demonstrated by Rubin *et al.* with structurally related fulleride based coinage metal complexes. However, this resulted in very large structures with atypically non-planar and highly conjugated Cp moieties.<sup>20</sup> As demonstrated in seminal works of Menjón and Dias, both  $\text{CF}_3$  ligands and organic ligands containing  $\text{CF}_3$  groups (*e.g.* scorpionates) are ideal to successfully stabilize coinage metal complexes in various oxidation states and coordination geometries.<sup>21–37</sup> As a consequence, we considered application of the perfluorinated Cp\* analogue  $[\text{C}_5(\text{CF}_3)_5]$ , whose initial coordination and reactivity was recently investigated.<sup>38–40</sup> Being sterically demanding, but also oxidatively stable, this Cp ligand appeared to be a suitable candidate for the elucidation of coinage metal Cp coordination chemistry.

## Results and discussion

To offer a structurally comparable series of  $[\text{M}(\text{C}_5(\text{CF}_3)_5)(\text{L})]$  ( $\text{M} = \text{Cu, Ag, Au}$ ) coinage metal complexes, a uniform composition with suitable co-ligands was envisaged. Previous works towards

<sup>a</sup>Freie Universität Berlin, Fabeckstraße 34/36, 14195 Berlin, Germany. E-mail: [moritz.maliszewski@fu-berlin.de](mailto:moritz.maliszewski@fu-berlin.de)

<sup>b</sup>Technische Universität Berlin, Straße des 17. Juni 135, 10623 Berlin, Germany

† Electronic supplementary information (ESI) available: Experimental, spectroscopic and computational details. CCDC 2309684–2309686. For ESI and crystallographic data in CIF or other electronic format see DOI: <https://doi.org/10.1039/d3sc06299f>



cyclopentadienyl coordination chemistry predominantly demonstrated stabilization by different phosphines such as, *e.g.*  $\text{PPh}_3$  for copper,<sup>2–9</sup> silver,<sup>10</sup> or gold.<sup>11–17</sup>

However, in this case synthetic efforts with  $\text{PPh}_3$  based precursors were unsuccessful, resulting in an undefined reaction mixture, containing product traces without any Cp coordination, such as  $[\text{Au}(\text{PPh}_3)_2][\text{C}_5(\text{CF}_3)_5]$ . In fact, the great oxidative stability of the  $[\text{C}_5(\text{CF}_3)_5]^-$  ligand is accompanied by a generally weakly bonding character, but also by pronounced  $\delta$ -acceptor properties,<sup>38</sup> compared to ordinary electron rich Cp ligands. Thus, the strongly electron donating and sterically demanding  $\text{P}^t\text{Bu}_3$  was considered as a suitable co-ligand instead. Due to the extraordinary acidity of  $\text{HC}_5(\text{CF}_3)_5$  ( $\text{pK}_a = -2.2$ )<sup>41,42</sup> which was *in situ* generated from  $[\text{NEt}_4][\text{C}_5(\text{CF}_3)_5]$  and  $\text{H}_2\text{SO}_4$ ,<sup>38,43–45</sup>  $[\text{M}(\text{P}^t\text{Bu}_3)(\text{OAc})]$  ( $\text{M} = \text{Cu, Ag, Au}$ ) complexes were used for coordination attempts, as the weaker acid  $\text{CH}_3\text{COOH}$  could easily be displaced and removed from the reaction mixture. Consequently, all  $[\text{M}(\text{C}_5(\text{CF}_3)_5)(\text{P}^t\text{Bu}_3)]$  complexes were successfully synthesized in quantitative yield, demonstrating the preparation of the first complete series in Cp coinage metal coordination chemistry (Scheme 1).

For  $[\text{Au}(\text{C}_5(\text{CF}_3)_5)(\text{P}^t\text{Bu}_3)]$  the NMR spectroscopic results are in agreement with expectations of a rotationally unhindered  $\text{P}^t\text{Bu}_3$  ligand. However, the  $^{19}\text{F}$  and  $^{13}\text{C}\{^1\text{H}\}$ NMR spectra mimic a  $\eta^5$ -coordination of  $[\text{C}_5(\text{CF}_3)_5]^-$  towards the Au(i) center with  $C_5$ -symmetry, due to the equivalence of its carbon and fluorine atoms. As all structurally characterized Au–Cp complexes are either definitely, or at least slightly distorted  $\eta^1$ -coordinated, this observation is readily explained by fast metallotropic shifts in solution.<sup>11–17</sup> Subsequently, it was possible to obtain colorless single crystals and the corresponding molecular structure in the solid state by slowly cooling solutions in *n*-pentane/*ortho*-difluorobenzene (*o*DFB) to  $-35\text{ }^\circ\text{C}$  (Fig. 1, right).  $[\text{Au}(\text{C}_5(\text{CF}_3)_5)(\text{P}^t\text{Bu}_3)]$  crystallizes in the triclinic  $P\bar{1}$  space group and indeed exhibits a distinct  $\eta^1$ -coordination towards the Au(i) center. The by far shortest distance of  $2.206(7)\text{ \AA}$  is obtained for the Au–C1  $\sigma$ -bond, while the further gold–carbon distances increase in a very symmetrical fashion, being  $2.754(7)$  or  $2.737(7)\text{ \AA}$  for Au–C2 and Au–C5 and  $3.400(7)$  or  $3.393(7)\text{ \AA}$  for Au–C3 and Au–C4 (Table 1, right). In contrast to some known Au–Cp complexes there is no evidence for any distortion towards  $\eta^2$ - or  $\eta^3$ -coordination.<sup>11–13,15,47</sup> Consequently, the Cp-ring is assumed to have lost its aromatic stabilization, as demonstrated also by the significantly elongated C1–C2, C3–C4 and C5–C1 bonds of  $1.468(10)$ ,  $1.423(12)$ , and  $1.442(10)\text{ \AA}$ ,

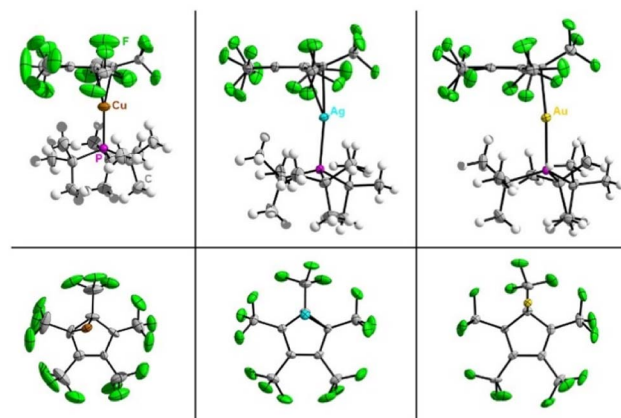
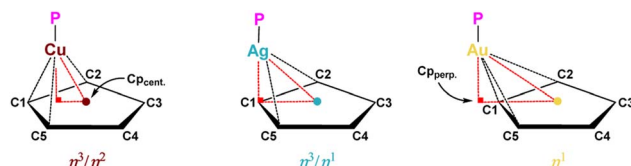


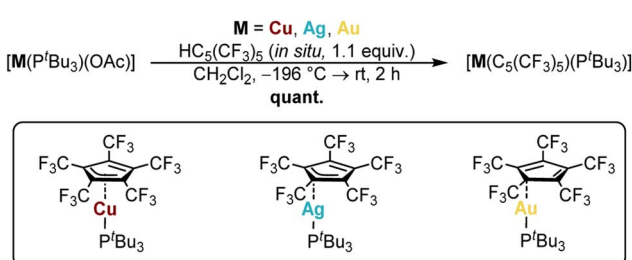
Fig. 1 Molecular structures in the solid state of  $[\text{M}(\text{C}_5(\text{CF}_3)_5)(\text{P}^t\text{Bu}_3)]$  ( $\text{M} = \text{Cu, Ag, Au}$ ), side-on view at the top and bottom view below. Disorder is omitted for clarity (see ESI, Fig. S31†). Ellipsoids are depicted with 50% probability level. Color code: white–hydrogen, grey–carbon, green–fluorine, purple–phosphorous, brown–copper, blue–silver, yellow–gold.

respectively. In contrast, the C2–C3 and C4–C5 bonds are shortened and close to regular unconjugated C=C double bonds, having  $1.383(9)$  and  $1.371(9)\text{ \AA}$ .<sup>48</sup> As a further consequence, the  $\sigma$ -bonded C1 shows a well pronounced pyramidalization. Therefore, the adjacent  $\text{CF}_3$ -group is significantly tilted out of the Cp-plane, with an  $\text{Cp}_{\text{cent.}}\text{–C1–CF}_3$  angle of  $148.37(58)^\circ$  ( $180^\circ$  for full planarity). The given hapticity is emphasized when

Table 1 Selected experimental distances [ $\text{\AA}$ ] (top) and angles [ $^\circ$ ] (bottom) for  $[\text{M}(\text{C}_5(\text{CF}_3)_5)(\text{P}^t\text{Bu}_3)]$  ( $\text{M} = \text{Cu, Ag, Au}$ ) and their respective hapticities



$[\text{M}(\text{C}_5(\text{CF}_3)_5)(\text{P}^t\text{Bu}_3)]$	Cu	Ag	Au
M–P	$2.201(15)$	$2.367(1)$	$2.268(2)$
M–C1	$2.119(6)$	$2.304(4)$	$2.206(7)$
M–C2	$2.589(10)$	$2.687(5)$	$2.754(7)$
M–C3	$2.947(8)$	$3.253(5)$	$3.400(7)$
M–C4	$2.803(8)$	$3.277(5)$	$3.393(7)$
M–C5	$2.299(6)$	$2.728(5)$	$2.737(7)$
C1–C2	$1.475(15)$	$1.429(6)$	$1.468(10)$
C2–C3	$1.401(8)$	$1.403(7)$	$1.383(9)$
C3–C4	$1.376(10)$	$1.412(6)$	$1.423(12)$
C4–C5	$1.412(9)$	$1.394(6)$	$1.371(9)$
C5–C1	$1.468(9)$	$1.439(6)$	$1.442(10)$
M–Cp <sub>cent.</sub>	$2.265(1)$	$2.609(1)$	$2.674(1)$
Cp <sub>cent.</sub> –Cp <sub>perp.</sub>	$0.871(7)$	$1.212(4)$	$1.541(6)$
P–M–C1	$167.80(18)$	$173.55(10)$	$175.98(18)$
C1–M–C2	$34.72(27)$	$32.11(13)$	$31.99(23)$
C1–M–C5	$38.54(22)$	$31.84(13)$	$32.16(22)$
M–C1–Cp <sub>cent.</sub>	$80.82(30)$	$90.31(22)$	$97.29(39)$
Cp <sub>cent.</sub> –C1–Cf <sub>3</sub>	$163.72(60)$	$157.63(40)$	$148.37(58)$



Scheme 1 Synthesis of  $[\text{M}(\text{C}_5(\text{CF}_3)_5)(\text{P}^t\text{Bu}_3)]$  from  $[\text{M}(\text{P}^t\text{Bu}_3)(\text{OAc})]$  and  $\text{HC}_5(\text{CF}_3)_5$  in quantitative yield ( $\text{M} = \text{Cu, Ag, Au}$ ).



comparing the relative position of the Au(i) center compared to the cyclopentadienyl ligand. Due to the mentioned  $\sigma$ -bonding, the orthogonal projection ( $Cp_{perp}$ ; see Table 1) of the gold atom is already located outside of the  $Cp$  plane giving a  $Cp_{cent.}-Cp_{perp}$  distance of 1.541(6) Å (for comparison  $C_{cent.}-C1 = 1.237(7)$  Å) and a significantly widened  $Au-C1-Cp_{cent.}$  angle of 97.29(39)°. The overall distortion is negligible given the very similar  $C1-Au-C2$  and  $C1-Au-C5$  angles of 31.99(23) and 32.16(22)°, respectively. These values were also verified by DFT structure optimizations ( $r^2$ SCAN-3c), providing an undistorted  $\eta^1$ -coordination with quite comparable values, as for example an  $Au-C1$  bond length of 2.214 Å and a  $Cp_{cent.}-C1-CF_3$  angle of 148° (see ESI, Table S4†).

[ $Ag(C_5(CF_3)_5)(P^tBu_3)$ ] represents a very rare example of  $Ag-Cp$  coordination without any supportive secondary coordinative interactions (as seen in, *e.g.*, [ $Ag(C_5(CO_2Me)_5)(PPh_3)$ ]).<sup>49</sup> Again, fast metallotropic shifts mimic a  $\eta^5$ -hapticity towards the  $Ag(i)$  center in the  $^{19}F$  and  $^{13}C\{^1H\}$  NMR spectra. Surprisingly, pronounced direct  $^{107}Ag$  ( $^1J_{P,Ag} = 651.6$  Hz) and  $^{109}Ag$  ( $^1J_{P,Ag} = 752.2$  Hz) coupling is visible in the  $^{31}P\{^1H\}$  spectrum, due to significant hindrance by the sterically demanding  $P^tBu_3$  ligand, resulting in two distinct doublets (absent for copper and gold).<sup>32,33</sup> This phenomenon is also observable by additional resonances in the  $^{13}C\{^1H\}$  spectrum, due to geminal and vicinal  $Ag(i)$  couplings. Single crystals were obtained by slow cooling of a [ $Ag(C_5(CF_3)_5)(P^tBu_3)$ ] solution in *n*-pentane/CH<sub>2</sub>Cl<sub>2</sub> to -75 °C. The corresponding molecular structure in the solid state revealed crystallization in the triclinic  $P\bar{1}$  space group (Fig. 1, middle). In contrast to [ $Ag(C_5(CF_3)_5)(P^tBu_3)$ ] the bonding situation is less definite. It shows a strong tendency towards  $\sigma$ -bonding ( $Ag-C1$  bond length 2.304(4) Å), but with some tilt towards alkene  $\pi$ -bonding (Table 1, middle). Here the  $Ag(i)$  center is slightly distorted, giving a shortened  $Ag-C2$  distance of 2.687(5) Å, while the  $Ag-C5$  distance is 2.728(5) Å, indicating secondary interactions. Consequently, the conjugation of the aromatic system is expected to be more pronounced. Indeed, the  $C2-C3$  and  $C4-C5$  bonds are significantly elongated, with 1.403(7) or 1.394(6) Å, and show less double-bond character compared to [ $Ag(C_5(CF_3)_5)(P^tBu_3)$ ]. In contrast,  $C1-C2$ ,  $C3-C4$  and  $C5-C1$  distances are shortened, with 1.429(6), 1.412(6) and 1.439(6) Å, respectively. Additionally, the  $Cp_{cent.}-C1-CF_3$  angle decreases to 157.63(40)°, indicating minor pyramidalization at  $C1$ . Considering the relative position of silver towards the cyclopentadienyl ligand a significant deviation from  $\eta^1$ -coordination is demonstrated. The  $Ag-C1-Cp_{cent.}$  angle reduces to 90.31(22)°, showing an almost perpendicular orientation of

silver towards  $C1$  and a strongly shortened  $Cp_{cent.}-Cp_{perp}$  distance of 1.212(4) Å compared to [ $Ag(C_5(CF_3)_5)(P^tBu_3)$ ]. Considering the comparable values for  $C1-Ag-C2$  and  $C1-Ag-C5$  angles of 32.11(13) and 31.84(13)°, asymmetric coordination patterns are excluded, and the bonding situation is properly described as  $\eta^3/\eta^1$  ( $\eta^3$  with significant distortion towards  $\eta^1$ ). These findings are further emphasized by our DFT structure optimizations ( $r^2$ SCAN-3c) of [ $Ag(C_5(CF_3)_5)(P^tBu_3)$ ], providing for example distances of 2.272, 2.698, and 2.719 Å for  $Ag-C1$ ,  $Ag-C2$ ,  $Ag-C5$ , respectively (see ESI, Table S4†). Compared to the structurally characterized [ $Ag(C_5(SiMe_3)_3H_2)(P^tBu_3)$ ], which exhibits either  $\eta^5$ - or  $\eta^3$ -hapticity,<sup>10</sup> the reduced  $\eta^3/\eta^1$ -hapticity of [ $Ag(C_5(CF_3)_5)(P^tBu_3)$ ] stands out and represents a so far unknown coordination mode for  $Ag-Cp$  complexes.

[ $Cu(C_5(CF_3)_5)(P^tBu_3)$ ], the last representative of the three coinage metal complexes, is again suggested to be  $\eta^5$ -coordinated by the  $^{19}F$  and  $^{13}C\{^1H\}$  NMR spectra. In contrast to gold and silver, a variety of exclusively  $\eta^5$ -coordinated monometallic  $Cu-Cp$  complexes is known.<sup>2-9</sup> Thus, the apparent  $C_5$  symmetry could not *a priori* be attributed to fast metallotropic shifts in solution, such as for [ $M(C_5(CF_3)_5)(P^tBu_3)$ ] ( $M = Ag, Au$ ). Single crystals and the corresponding molecular structure in the solid state were obtained from solutions of [ $Cu(C_5(CF_3)_5)(P^tBu_3)$ ] in *n*-pentane/CH<sub>2</sub>Cl<sub>2</sub>, slowly cooled to -75 °C (Fig. 1, left). [ $Cu(C_5(CF_3)_5)(P^tBu_3)$ ] crystallizes in the monoclinic  $P2_1/n$  space group and surprisingly did not exhibit  $\eta^5$ -bonding. Instead,  $[C_5(CF_3)_5]^-$  binds in a highly unsymmetrical fashion to the  $Cu(i)$  center, with a  $Cu-C1$  bond length of about 2.119(6) Å, and  $Cu-C2$  and  $Cu-C5$  distances of 2.589(10) or 2.299(11) Å, respectively (Table 1, left). This trend continues for the remote carbon atoms, as shown by  $Cu-C3$  and  $Cu-C4$  of 2.947(8) and 2.803(8) Å, respectively. Similar to the  $Cu-C$  distances, the  $C-C$  bond length vary strongly but still support the trend of a decreasing  $\sigma$ -bonding character compared to the heavier homologues and pronounced conjugation within the ligand. This is shown by the slightly elongated  $C2-C3$  and  $C4-C5$  bonds (1.401(8) and 1.412(9) Å), but also by the diminished  $Cp_{cent.}-C1-CF_3$  angle of 163.72(60)°, indicating less pyramidalization at  $C1$ . Regarding the relative position of copper towards the cyclopentadienyl ligand, the given trend of gold and silver is continued. The reduced  $Cu-C1-Cp_{cent.}$  angle of 80.82(30)° and a shortened  $Cp_{cent.}-Cp_{perp}$  distance of 0.871(7) Å show the orthogonal projection of copper to be distinctly located within the  $Cp$  plane. However, in contrast to [ $Ag(C_5(CF_3)_5)(P^tBu_3)$ ] and [ $Ag(C_5(CF_3)_5)(P^tBu_3)$ ] and as already indicated by the  $Cu-C$  bond lengths, the  $C1-Cu-C2$  and  $C1-Cu-C5$  angles differ significantly, being 34.72(27) and 38.54(22)°, respectively. These findings clearly exclude symmetric coordination modes and affirm a highly unusual coordination motif, describable as  $\eta^3/\eta^2$  ( $\eta^3$  with significant distortion towards  $\eta^2$ ). Except for two exotic examples of heterobimetallic complexes this is the only known  $Cu-Cp$  complex known without the common  $\eta^5$ -coordination.<sup>18,19</sup> Unfortunately, the overall data quality of the copper structure suffered from significant crystallographic disorder. However, the absence of a  $\eta^5$ -coordination was also demonstrated by structure optimizations ( $r^2$ SCAN-3c) of the complex, providing a very similar distorted  $\eta^3$ -coordination

**Table 2** Contributions to the binding energy [ $\text{kJ mol}^{-1}$ ] between a  $[Cu-PM_3]^+$  and a  $[C_5(CX_3)_5]^-$  ( $X = H, F$ ) fragment at the scalar relativistic ZORA- $r^2$ SCAN-3c level

$[C_5(CX_3)_5]^-$	$\Delta E_{\text{Pauli}}$	$\Delta E_{\text{Elstat.}}$	$\Delta E_{\text{Orb.Int.}}$	$\Delta E_{\text{Total}}$
X = H ( $\eta^5$ )	457.9	-826.2	-375.3	-750.2
X = H ( $\eta^3/\eta^1$ )	386.9	-783.1	-305.3	-710.1
X = F ( $\eta^5$ )	441.8	-623.3	-311.7	-502.8
X = F ( $\eta^3/\eta^1$ )	349.5	-587.5	-253.2	-502.4



with Cu–C1, Cu–C2 and Cu–C5 distances of 2.057, 2.502 and 2.201 Å, respectively (see ESI, Table S4†).

The unusual stability of the prepared  $[M(C_5(CF_3)_5)(P^tBu_3)]$  ( $M = Cu, Ag, Au$ ) coinage metal complexes is particularly intriguing. While most Au–Cp complexes such as  $[Au(C_5Ph_4H)(PPh_3)]$  show significant air sensitivity,<sup>11</sup> and the sterically less shielded  $[Au(C_5H_5)(PPh_3)]$  additionally thermal lability at room temperature,<sup>50</sup>  $[Au(C_5(CF_3)_5)(P^tBu_3)]$  decomposes only slowly at ambient conditions. It is even more fascinating that  $[Ag(C_5(CF_3)_5)(P^tBu_3)]$  is not only thermostable and relatively insensitive against air, but it is also storable without the exclusion of light. The structurally non-characterized  $[Ag(C_5H_5)(PPh_3)]$  in contrast decomposes within minutes at room temperature under an argon atmosphere.<sup>51,52</sup>  $[Cu(C_5(CF_3)_5)(P^tBu_3)]$  is also significantly more stable than related Cu–Cp complexes, which often have pronounced sensitivity against air.<sup>2,4,7</sup> By displaying the space-filling van der Waals spheres of  $[M(C_5(CF_3)_5)(P^tBu_3)]$  ( $M = Cu, Ag, Au$ ), the relevant steric demand becomes apparent for both  $[C_5(CF_3)_5]^-$  and  $P^tBu_3$  (see ESI, Fig. S34†). Pronounced shielding of the coinage metal centers is observed, which is thought to partly suppress decomposition reactions. However, the spatial demand is only minor compared to the outstandingly well shielded fulleride complexes of Rubin *et al.*, and stabilization of these coinage metal complexes by sterical shielding alone appears insufficient.<sup>20</sup>  $[C_5(CF_3)_5]^-$  offers the additional advantage of an extraordinarily high electron affinity and oxidative stability, showing a calculated ionization energy of 4.84 eV compared to only 1.73 eV for  $[C_5H_5]^-$  (at the PNO-CCSD(T)-F12b/cc-pVTZ-F12//r<sup>2</sup>SCAN-3c level, the value for  $[C_5H_5]^-$  agrees very well with high-quality estimates of 1.79 eV<sup>53</sup>) Thus, even coordination chemistry with highly oxidative metal centers, such as Ag(i) and Au(i) is feasible, and oxidative decomposition pathways involving single-electron transfer are effectively impeded.

To further understand the trends in bonding between the  $[C_5(CF_3)_5]^-$  ligand and the coinage metals, scalar-relativistic ZORA-r<sup>2</sup>SCAN-3c<sup>54</sup> DFT calculations have been carried out. To allow for a simpler analysis, we replaced the 'Bu groups of the phosphine ligand by methyl groups. While the effects of this truncation on the bond lengths are only minor in the Au and Ag complexes, the differences become significant in the Cu complex, reducing the Cu–C3 and Cu–C2 distance by about 0.152 and 0.173 Å, respectively (see ESI, Table S6†). The obtained structure is then very similar to that of the Ag complex, which indicates that the experimentally observed differences between the Ag and the Cu complexes are to a large extent due to secondary interactions between the 'Bu groups of the phosphine and the CF<sub>3</sub> groups of the Cp ligand in the copper case. These interactions are much less pronounced in the silver and gold complexes due to the larger metal-to-ligand distances (see Table 1). The remaining difference between the Ag and the Au complexes can be explained by the well-known, enhanced covalency of Au–C bonds due to the relativistic stabilization and contraction of the 6s orbitals.<sup>55–58</sup> This effect can also be observed in the charges obtained from natural population analysis (NPA; see ESI, Table S8†). Removing scalar relativistic effects from the calculation results in all three metal centers

exhibiting almost identical  $\eta^3/\eta^1$  coordination motifs (see ESI, Table S7†).

This leaves the question, why all these metal centers, and especially copper prefer such a coordination motif, in contrast to the typically observed  $\eta^5$ -coordination for Cp or Cp\*. Using the PMe<sub>3</sub> model systems, we find that the standard Cp\* ligand indeed prefers a fivefold coordination, which means that the origin of the uncommon motif is due to the unique electronic properties of  $[C_5(CF_3)_5]^-$ . For a closer analysis, we have obtained  $\eta^5$  and  $\eta^3/\eta^1$  structures of the  $[C_5(CF_3)_5]^-$  and Cp\* systems, respectively, by replacing CH<sub>3</sub> groups by CF<sub>3</sub> groups (and *vice versa*) in the minimum structures and re-optimizing the complexes while freezing the C<sub>5</sub> core and the M–PMe<sub>3</sub> unit. Using these four structures, we have performed standard energy decomposition analyses (EDA)<sup>59</sup> for the bonding between a  $[Cu(PMe_3)]^+$  and a  $[C_5(CX_3)_5]^-$  (X = H, F) fragment (Table 2). While the Cp\* ligand has a clear preference of 40 kJ mol<sup>-1</sup> for  $\eta^5$  coordination, the difference practically vanishes for  $[C_5(CF_3)_5]^-$ . These preferences translate into the total energy differences, where  $[Cu(C_5(CF_3)_5)(PMe_3)]$  prefers the  $\eta^3/\eta^1$  motif by 11 kJ mol<sup>-1</sup>, while the preference of  $[Cu(C_5(CH_3)_5)(PMe_3)]$  for the  $\eta^5$  structure is three times larger (32 kJ mol<sup>-1</sup>). In a  $\eta^3/\eta^1$  structure, we find overall reduced interactions between the fragments. This is true both for the destabilizing Pauli-repulsion ( $\Delta E_{Pauli}$ ) and the stabilizing electrostatic ( $\Delta E_{Elstat}$ ) and orbital-interaction ( $\Delta E_{Orb.Int.}$ ) terms. For the Cp\* ligand these lowered interactions are unfavorable, as the increase in stabilization in a  $\eta^5$  structure outweighs the increased Pauli-repulsion. For the  $[C_5(CF_3)_5]^-$  ligand, this is no longer the case. Here, the reduction in Pauli-repulsion with lower coordination number is significantly larger than for the Cp\* ligand. At the same time, the gain in orbital interaction energies in an  $\eta^5$  binding motif is reduced for  $[C_5(CF_3)_5]^-$  due to its decreased donor ability.<sup>38</sup> For the Ag complexes, the analogous results are provided in Table S9,† showing a qualitatively similar picture but a clearer preference for the  $\eta^3/\eta^1$  motif with  $[C_5(CF_3)_5]^-$ . We note in passing that, unlike  $[C_5H_5]^-$ , the structure of the free  $[C_5(CF_3)_5]^-$  ligand appears to be slightly non-planar due to hyperconjugation and pyramidalization effects of the negative charge.<sup>60,61</sup> The corresponding energy differences are, however, small compared to the interaction energies in the metal complexes.

## Conclusions

Due to the extraordinarily high electron affinity and oxidative stability of  $[C_5(CF_3)_5]^-$  it was possible to prepare the first complete and structurally comparable series of cyclopentadienyl coinage metal coordination species. All coinage metal complexes  $[M(C_5(CF_3)_5)(P^tBu_3)]$  ( $M = Cu, Ag, Au$ ) were structurally characterized<sup>62</sup> and revealed distinct coordination modes, with hapticities ranging from  $\eta^1$ ,  $\eta^3/\eta^1$  to  $\eta^3/\eta^2$  for gold, silver and copper, respectively. In contrast to earlier experience, these coinage metal Cp complexes demonstrated not only significant stability at room temperature, but also towards moisture, air and light. Quantum-chemical calculations support the coordination motifs observed in the crystal



structures, connecting them to the specific electronic structure of the new ligand system arising from the extremely electron-withdrawing  $\text{CF}_3$ -substituents.

## Data availability

Data supporting this manuscript is available within the ESI<sup>†</sup> and available on request.

## Author contributions

RS: investigation, formal analysis, writing (original draft); MR: investigation, formal analysis, writing (original draft); NGK: investigation; SMR: formal analysis; MK: supervision, writing (review and editing); MM: conceptualization, supervision, project administration, writing (review and editing).

## Conflicts of interest

There are no conflicts to declare.

## Acknowledgements

Gefördert durch die Deutsche Forschungsgemeinschaft (DFG) – Projektnummer 387284271 – SFB 1349. Computing time was made available by High-Performance Computing at ZEDAT/FU Berlin. The authors acknowledge the assistance of the Core Facility BioSupraMol supported by the DFG. Robin Sievers thanks the Fonds of the Chemical Industry (FCI) for a Kekulé PhD Fellowship.

## Notes and references

- 1 C. R. Groom, I. J. Bruno, M. P. Lightfoot and S. C. Ward, *Acta Crystallogr., Sect. B: Struct. Sci., Cryst. Eng. Mater.*, 2016, **72**, 171–179.
- 2 G. Wilkinson and T. S. Piper, *J. Inorg. Nucl. Chem.*, 1956, **2**, 32–37.
- 3 F. A. Cotton and T. J. Marks, *J. Am. Chem. Soc.*, 1969, **91**, 7281–7285.
- 4 F. A. Cotton and J. Takats, *J. Am. Chem. Soc.*, 1970, **92**, 2353–2358.
- 5 L. T. Delbaere, D. W. McBride and R. B. Ferguson, *Acta Crystallogr., Sect. B: Struct. Crystallogr. Cryst. Chem.*, 1970, **26**, 515–521.
- 6 T. P. Hanusa, T. A. Ulibarri and W. J. Evans, *Acta Crystallogr., Sect. C: Cryst. Struct. Commun.*, 1985, **41**, 1036–1038.
- 7 Q. T. Anderson, E. Erkizia and R. R. Conry, *Organometallics*, 1998, **17**, 4917–4920.
- 8 G. A. Carriedo, J. A. K. Howard and F. G. A. Stone, *Dalton Trans.*, 1984, 1555–1561.
- 9 C. Zybill and G. Müller, *Organometallics*, 1987, **6**, 2489–2494.
- 10 H. G. Stammller, P. Jutzi, W. Wieland and B. Neumann, *Acta Crystallogr., Sect. C: Cryst. Struct. Commun.*, 1998, **54**, IUC9800064.
- 11 E. G. Perelova, K. J. Grandberg, V. P. Dyadchenko and T. V. Baukova, *J. Organomet. Chem.*, 1981, **217**, 403–413.
- 12 M. I. Bruce, J. K. Walton, B. W. Skelton and A. H. Wheite, *Dalton Trans.*, 1983, 809–814.
- 13 H. Werner, H. Otto, T. Ngo-Khac and C. Bruschka, *J. Organomet. Chem.*, 1984, **262**, 123–136.
- 14 Y. T. Struchkov, Y. L. Slovokhotov, L. Yu, D. N. Kravtsov, T. V. Baukova, E. G. Perelova and K. J. Grandberg, *J. Organomet. Chem.*, 1988, **338**, 269–280.
- 15 H. Schumann, F. H. Görlitz and A. Dietrich, *Chem. Ber.*, 1989, **122**, 1423–1426.
- 16 M. I. Bruce, P. A. Humphrey, M. L. Williams, B. W. Skelton and A. H. White, *Aust. J. Chem.*, 1989, **42**, 1847–1857.
- 17 L. G. Kz'mina, A. V. Churakov, K. I. Grandberg and V. S. Kuz'min, *Koord. Khim.*, 1997, **23**, 170–176.
- 18 N. Martínez-Espada, M. Mena, M. E. G. Mosquera, A. Pérez-Redondo and C. Yélamos, *Organometallics*, 2010, **29**, 6732–6738.
- 19 R. Batcup, F. S. N. Chiu, V. T. Annibale, J. E. U. Huh, R. Tan and D. Song, *Dalton Trans.*, 2013, 16343–16350.
- 20 H. Halim, R. D. Kennedy, M. Suzuki, S. I. Khan, P. L. Diaconescu and Y. Rubin, *J. Am. Chem. Soc.*, 2011, **133**, 6841–6851.
- 21 S. Martínez-Salvador, J. Forniés, A. Martín and B. Menjón, *Angew. Chem., Int. Ed.*, 2011, **50**, 6571–6574.
- 22 S. Martínez-Salvador, L. R. Falvello, A. Martín and B. Menjón, *Chem.-Eur. J.*, 2013, **19**, 14540–14552.
- 23 A. Pérez-Bitrián, M. Baya, J. M. Casas, L. R. Falvello, A. Martín and B. Menjón, *Chem.-Eur. J.*, 2017, **23**, 14918–14930.
- 24 D. Joven-Sancho, M. Baya, A. Martín and B. Menjón, *Chem.-Eur. J.*, 2018, **24**, 13098–13101.
- 25 D. Joven-Sancho, M. Baya, A. Martín, J. Orduna and B. Menjón, *Chem.-Eur. J.*, 2020, **26**, 4471–4475.
- 26 D. Joven-Sancho, L. Demonti, A. Martín, N. Saffon-Merceron, N. Nebra, M. Baya and B. Menjón, *Chem. Commun.*, 2023, **59**, 4166–4168.
- 27 A. Pérez-Bitrián, S. Alvarez, M. Baya, J. Echeverría, A. Martín, J. Orduna and B. Menjón, *Chem.-Eur. J.*, 2023, **29**, e202203181.
- 28 J. S. Lakhi, M. R. Patterson and H. V. R. Dias, *New J. Chem.*, 2020, **44**, 14814–14822.
- 29 H. V. R. Dias, C. S. P. Gamage, N. B. Jayaratna and C. V. Hettiarachchi, *New J. Chem.*, 2020, **44**, 17079–17087.
- 30 M. Vanga, A. Noonikara-Poyil, J. Wu and H. V. R. Dias, *Organometallics*, 2022, **41**, 1249–1260.
- 31 M. Vanga, A. Muñoz-Castro and H. V. R. Dias, *Dalton Trans.*, 2022, **51**, 1308–1312.
- 32 W. Jin, H. J. Kim, H. L. Lu and H. V. R. Dias, *Inorg. Chem.*, 1996, **35**, 2317–2328.
- 33 S. Singh and H. V. R. Dias, *Inorg. Chem.*, 2004, **43**, 7396–7402.
- 34 J. Mehara, B. T. Watson, A. Noonikara-Poyil, A. O. Zacharias, J. Roithová and H. V. R. Dias, *Chem.-Eur. J.*, 2022, **28**, e202103984.
- 35 R. G. Browning, S. A. Richey, C. J. Lovely and H. V. R. Dias, *Organometallics*, 2004, **23**, 1200–1202.
- 36 G. Wang, A. Noonikara-Poyil, I. Fernández and H. V. R. Dias, *Chem. Commun.*, 2022, **58**, 3222.



37 M. Vanga, A. Muñoz-Castro and H. V. R. Dias, *Chem.-Eur. J.*, 2023, e202303339.

38 R. Sievers, M. Sellin, S. M. Rupf, J. Parche and M. Malischewski, *Angew. Chem., Int. Ed.*, 2022, e202211147.

39 J. Parche, S. M. Rupf, R. Sievers and M. Malischewski, *Dalton Trans.*, 2023, **52**, 5496–5502.

40 R. Sievers, J. Parche, N. G. Kub and M. Malischewski, *Synlett*, 2023, **34**, 1079–1086.

41 G. Paprott and K. Seppelt, *J. Am. Chem. Soc.*, 1984, **106**, 4061–4062.

42 E. D. Laganis and D. M. Lemal, *J. Am. Chem. Soc.*, 1980, **102**, 6633–6634.

43 R. D. Chambers, S. J. Mullins, A. J. Roche and J. F. S. Vaughan, *Chem. Commun.*, 1995, 841–842.

44 R. D. Chambers, A. J. Roche and J. F. S. Vaughan, *Can. J. Chem.*, 1996, **74**, 1925–1929.

45 R. Alberto, personal communication.

46 R. G. Goel and P. Pierre, *Inorg. Chem.*, 1978, **17**, 2876–2879.

47 T. V. Baukova, Y. L. Slovokhotov and Y. T. Struchkov, *J. Organomet. Chem.*, 1981, **220**, 125–137.

48 D. R. Lide, *Tetrahedron*, 1962, **17**, 125–134.

49 M. I. Bruce, M. L. Williams, B. W. Skelton and A. H. White, *Dalton Trans.*, 1983, 799–808.

50 R. Hüttel, U. Raffay and H. Reinheimer, *Angew. Chem.*, 1967, **19**, 859–860.

51 H. K. Hofstee, J. Boersma and G. J. M. van der Kerk, *J. Organomet. Chem.*, 1976, **120**, 313–317.

52 D. W. Macomber and M. D. Rausch, *J. Am. Chem. Soc.*, 1983, **105**, 5325–5329.

53 P. K. Lo and K. C. Lau, *J. Phys. Chem.*, 2014, **118**, 2498–2507.

54 T. Gasevic, J. B. Stückrath, S. Grimme and M. Bursch, *J. Phys. Chem.*, 2022, **23**, 3826–3838.

55 P. Pykkö, *Chem. Rev.*, 1988, **88**, 563–594.

56 P. Pykkö, *Angew. Chem., Int. Ed.*, 2004, **43**, 4412–4456.

57 P. Pykkö, *Inorg. Chim. Acta*, 2005, **358**, 4113–4130.

58 P. Pykkö, *Chem. Soc. Rev.*, 2008, **37**, 1967–1997.

59 T. Ziegler and A. Rauk, *Theor. Chim. Acta*, 1977, **46**, 1–10.

60 J. I. Wu, F. A. Evangelista and P. v. R. Schleyer, *Org. Lett.*, 2010, **12**, 768–771.

61 W. T. Borden, *Chem. Commun.*, 1998, 1919–1925.

62 Deposition Numbers 2309684–2309686 contain the supplementary crystallographic data for this paper.

